AD-A282 090

‖‖‖‖‖‖‖‖‖‖‖‖‖‖‖‖‖‖‖‖

REPORT DOCUMENTATION PAGE

Public reporting burden for this collection of information is estimated to average 1 hour per response, including the time for reviewing instructions, searching existing data sources, gathering and maintaining the data needed, and completing and reviewing the collection of information. Send comments regarding this burden estimate or any other aspect of this collection of information, including suggestions for reducing this burden, to Washington Headquarters Services, Directorate for Information Operations and Reports, 1215 Jefferson Davis Highway, Suite 1204, Arlington, VA 22202-4302, and to the Office of Management and Budget, Paperwork Reduction Project (0704-0188), Washington, DC 20503

1 AGENCY USE ONLY (Leave blank)	2 REPORT DATE	3 REPORT TYPE AND DATES COVERED
	June 1994	Professional Paper

4 TITLE AND SUBTITLE	5. FUNDING NUMBERS
EFFICACY OF FREQUENCY ON DETECTING TARGETS IN FOLIAGE USING INCOHERENT CHANGE DETECTION	PR: CD36
6. AUTHOR(S)	PE: 0603226E
R. R. James and C. R. Hendrickson	WU: DN302002

7. PERFORMING ORGANIZATION NAME(S) AND ADDRESS(ES)	8. PERFORMING ORGANIZATION REPORT NUMBER
Naval Command, Control and Ocean Surveillance Center (NCCOSC) RDT&E Division San Diego, CA 92152-5001	

9. SPONSORING/MONITORING AGENCY NAME(S) AND ADDRESS(ES)	10. SPONSORING/MONITORING AGENCY REPORT NUMBER
Advanced Research Project Agency 3701 North Fairfax Drive Arlington, VA 22203	

11. SUPPLEMENTARY NOTES

JUL 2 2 1994

12a. DISTRIBUTION/AVAILABILITY STATEMENT

Approved for public release; distribution is unlimited.

12b. DISTRIBUTION

94-22368

‖‖‖‖‖‖‖‖‖‖‖‖‖‖

13. ABSTRACT *(Maximum 200 words)*

The effectiveness of applying incoherent change detection to multipass synthetic aperture radar (SAR) images and targets in foliage is affected by the operating radar frequency band. Incoherent change detection is achieved by taking the weighted difference of the magnitude of two well registered passes of SAR imagery. Items which change between two passes, such as a target present in the first pass and not present in the second pass, will appear in the weighted difference image. With well registered wideband SAR imagery, images can be divided into frequency bands and evaluated using incoherent change detection. An Environmental Research Institute of Michigan (ERIM) Rail SAR experiment provides such a data collection. The Rail SAR is characterized by polarimetric, wideband (400 MHz -1.3 GHz), multipass (with and without targets), well registered SAR images. The ERIM Rail SAR data is divided into a number of frequency bands which simulate the high-band Stanford Research Institute, International (SRI) Ultra-WideBand Radar (UWBR) (350-550 MHz), the Loral miniature SAR (MSAR) (500-800 MHz), and the Naval Air Warfare Center (NAWC) P-3 upgraded UWBR (200-900 MHz) sensor. This paper shows how these sensors work on targets in foliage using incoherent change detection and provides an experimental measurement of upper-bound performance.

DTIC QUALITY INSPECTED 5

Published in *SPIE*, vol. 2230, pp. 220-229, April 1994.

14 SUBJECT TERMS		15 NUMBER OF PAGES
data fusion digital terrain elevations paragon computer	recognition synthetic aperture radar target detection	
		16 PRICE CODE

17. SECURITY CLASSIFICATION OF REPORT	18 SECURITY CLASSIFICATION OF THIS PAGE	19 SECURITY CLASSIFICATION OF ABSTRACT	20 LIMITATION OF ABSTRACT
UNCLASSIFIED	UNCLASSIFIED	UNCLASSIFIED	SAME AS REPORT

21a NAME OF RESPONSIBLE INDIVIDUAL	21b TELEPHONE *(include Area Code)*	21c OFFICE SYMBOL
R. R. James	(619) 553-6131	Code 844

Accession For

NTIS GRA&I	☑	
DTIC TAB	☐	
Unannounced	☐	
Justification		

By_____
Distribution/_____

Availability Codes

Dist	Avail and/or Special
A-1	20

Efficacy of frequency on detecting targets in foliage using incoherent change detection

Robert R. James and Clark R. Hendrickson

Naval Command, Control and Ocean Surveillance Center
Research, Development, Test, and Evaluation Division
53490 Dow Street, Room 132
San Diego, California 92152

ABSTRACT

The effectiveness of applying incoherent change detection to multipass synthetic aperture radar (SAR) images and targets in foliage is affected by the operating radar frequency band. Incoherent change detection is achieved by taking the weighted difference of the magnitude of two well registered passes of SAR imagery. Items which change between two passes, such as a target present in the first pass and not present in the second pass, will appear in the weighted difference image. With well registered wideband SAR imagery, images can be divided into frequency bands and evaluated using incoherent change detection. An Environmental Research Institute of Michigan (ERIM) Rail SAR experiment provides such a data collection. The Rail SAR is characterized by polarimetric, wideband (400 MHz - 1.3 GHz), multipass (with and without targets), well registered SAR images. The ERIM Rail SAR data is divided into a number of frequency bands which simulate the high-band Stanford Research Institute, International (SRI) Ultra-WideBand Radar (UWBR) (350-550 MHz), the Loral miniature SAR (MSAR) (500-800 MHz), and the Naval Air Warfare Center (NAWC) P-3 upgraded UWBR (200-900 MHz) sensor. This paper shows how these sensors work on targets in foliage using incoherent change detection and provides an experimental measurement of upper-bound performance.

1. INTRODUCTION

The Advanced Research Projects Agency (ARPA) Surveillance and Targeting portion of the War Breaker program has been interested in using SAR for detecting targets obscured by foliage. To penetrate the foliage and uncover the presence of targets necessitates the use of portions of the Very High Frequency (VHF)/ Ultra High Frequency (UHF) bands.[1] ARPA has been sponsoring collection of foliage penetration (FOPEN) data using existing sensors of limited capability. As a result, ARPA is supporting the development of new FOPEN sensors which will provide improved capability and performance. Before these sensors come on-line and are available for data collection, a prediction of their capabilities would be desirable. Under the Air Force Concealed Target Detection (CTD) program, ERIM has conducted a Rail SAR experiment looking for targets obscured by foliage.[2] The ERIM Rail SAR experiment was conducted in such a manner that a number of FOPEN sensors could be evaluated for detecting an obscured target and by employing incoherent change detection. The ERIM Rail SAR configuration records data polarimetric (HH and VV) and over a wideband (400-1300 MHz). Scenes were recorded once with an obscured target present and then with the target removed. Two particular scenes are described and evaluated. Each of these scenes is converted to the spectral domain. The images are spectrally filtered to represent three sensors: (1) SRI UWBR, (2) Loral MSAR, and NAWC P-3 SAR. After conversion back to the spatial domain, the images are normalized and compared through the use of incoherent change detection. A number of observations are then discussed.

2. RAIL SAR DESCRIPTION AND EXPERIMENT CONFIGURATION

Figure 1 shows the ERIM Rail SAR as it appears at the experimental test site.[3] The Rail SAR consists of two perpendicular horn antennas (vertical and horizontal), mounted and scanned over a 10-meter horizontal rail. The rail can be raised between 3 meters and 14 meters. This provided a 30-degree depression angle to the center of the scene. The frequency response of the Rail SAR is 400-1300 MHz. This allowed a range resolution of 0.167meters and an azimuth resolution of 0.5 meters.

Figure 1. ERIM Rail SAR in the field at the experimental site.

Because the Rail SAR is a ground-based system and images are recorded in the near field, ERIM performed plane wave decomposition to make the data look as if it were recorded in the far field. Then traditional spotlight SAR processing was applied to form the image. A full-band image scene is represented by 240-complex in-phase and quadrature pixels in the range direction and 300-complex in-phase and quadrature pixels in the azimuth direction. Each range pixel spacing is roughly 0.167 meters and each azimuth pixel spacing is 0.1 meters (5 times oversampled). This results in a scene size of roughly 40 meters in range by 30 meters in azimuth. For the processing done in this paper, the near-range (top 25 azimuth lines) and the far-range (bottom 25 azimuth lines) were removed.

Figure 2 depicts the experimental layout. At the edge of a hardwood forest and within the center of a 20 meter by 20 meter scene, a truck is placed. Corner reflectors were placed at the positions indicated. The two near range corner reflectors were 42-inch trihedrals and the far range reflector was a 5.6-foot trihedral. Both the corner reflectors and vehicle were obscured by the foliage. Figure 3 shows a ground level view of the obscured truck at broadside. The Rail SAR was positioned at three locations relative to the truck; (1) 24-degrees left of broadside, broadside, 24-degrees right of broadside. Figure 4 shows the Rail SAR perspective looking into the hardwood forest with the obscured vehicle in the center of the scene and at broadside. A combination of experiments were conducted by recording the scene with the truck and corner reflectors present and then removed. Not all possible configurations were recorded. When the Rail SAR was positioned off of broadside the corner reflectors were rotated so as to appear broadside to the Rail SAR.

Two experimental configurations are analyzed in this paper. The first scene looks at the obscured vehicle 24-degrees left of broadside and with the corner reflectors present. The second scene looks at the same area as seen by scene 1 except the vehicle and corner reflectors are removed. Scene 1 (truck and corner reflectors) was collected at 15:30 on 31 August 1992 and took roughly 19 minutes. Scene 2 (clutter only) was collected at 16:18 on 1 September 1992 and took roughly 20 minutes.
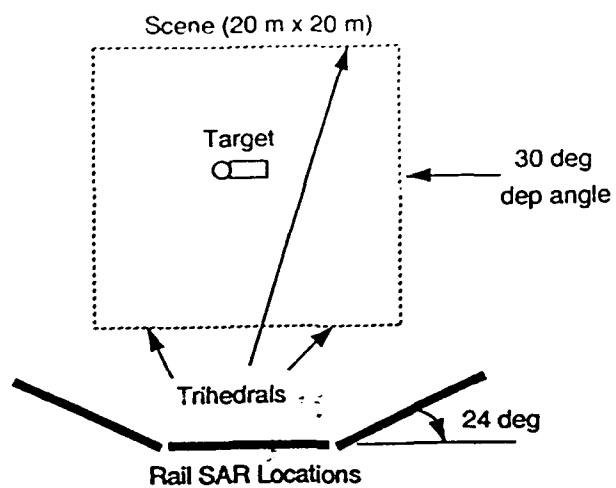
Figure 2. Experimental Layout.

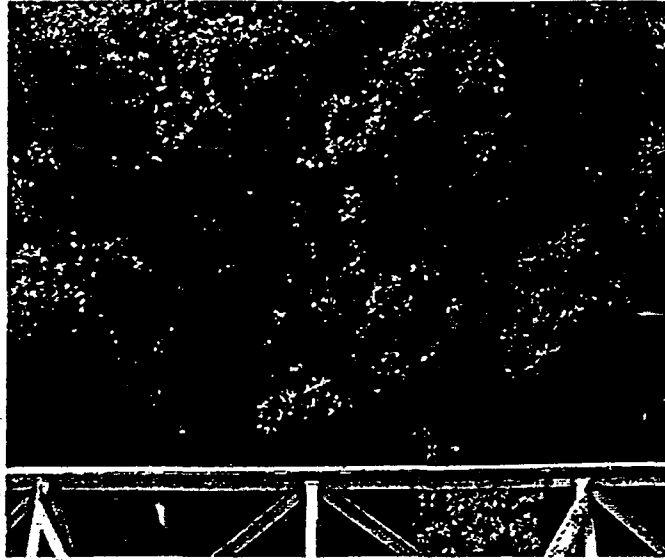Figure 3. Ground level look of obscured vehicle (truck).

Figure 4. Rail SAR perspective looking at the obscured vehicle in the broadside position.

3. SENSOR DESCRIPTION

Three SAR platforms are considered in this analysis. These include the SRI International UWBR, the Loral MSAR, and NAWC P-3 upgraded UWB SAR. The following is a summary of the characteristics of these sensors.

3.1. SRI UWBR

The SRI International Ultra Wideband Radar (UWBR) is a single frequency, HH-polarization impulse radar that operates on a Beech Queen Air aircraft. The sensor operates in a frequency band covering 100 to 550 MHz. Four center frequencies are selectable including 200, 300, 400, and 450 MHz. A single pulse transmit waveform allows for a 200 MHz bandwidth and gives a range and azimuth resolution of 1 meter by 1 meter. Most data is recorded in the 300 MHz mode to minimize RFI. For this analysis, the upper operating frequency band, 350 to 550 MHz will be simulated. Although the ERIM Rail SAR lower cut-off frequency is 400 MHz, the upper band of the SRI sensor will be simulated by an operating frequency range of 400 to 600 MHz.

3.2. Loral MSAR

The Loral miniature synthetic aperture radar (MSAR) is a multiple-polarization instrument that operates on a Beech aircraft. It uses a swept frequency radar and operates in the 500 to 800 MHz band. The effective range and azimuth resolution is 0.5 meter by 0.5 meter. The antenna includes a wide-angle, quad-ridge horn looking out the side door of the aircraft. The Loral MSAR sensor will be simulated by using the 500 to 800 MHz operating band of the ERIM Rail SAR.

3.3. NAWC P-3 upgraded UWB SAR

The NAWC P-3 sensor is a multiple-frequency, multiple-polarization SAR instrument which operates on a U.S. Navy P-3 aircraft. At present, ERIM is providing instrumentation which will upgrade the P-3 to include multi-polarization, VHF/UHF SAR capability over the 200 to 900 MHz band. Roughly 550 to 600 MHz of effective bandwidth will be used. This gives a resolution of approximately 0.3 meters. To simulate the P-3 using the ERIM Rail SAR, a 600 MHz bandwidth is assumed and will cover 400 to 1000 MHz.

4. SENSOR SIMULATION PROCEDURE

The most accurate way to simulate the effects of the airborne sensors is to frequency filter the preformed images. This data was not available. Without access to the preformed image data, the images must be converted from the spatial domain to the spectral domain, frequency filtered, and converted back to the spatial domain. After zero padding the spatial image (190 by 300 pixels) to 512 by 512 pixels, a 2-dimensional (2-D) complex fast fourier transform (FFT) is applied. Figure 5 shows on the left the intensity (linear scale) of the clutter only image (30 meters by 30 meters), and on the right the intensity (linear scale) of the 2D complex FFT image. The sensor is looking from bottom to top (corresponding to the layout in figure 2). Rings of constant frequency are shown on the right side of figure 5, ranging from 400 MHz (nearest the bottom) to 1300 MHz (closes to the top). Notice the aliasing on the left and right edges of the image.
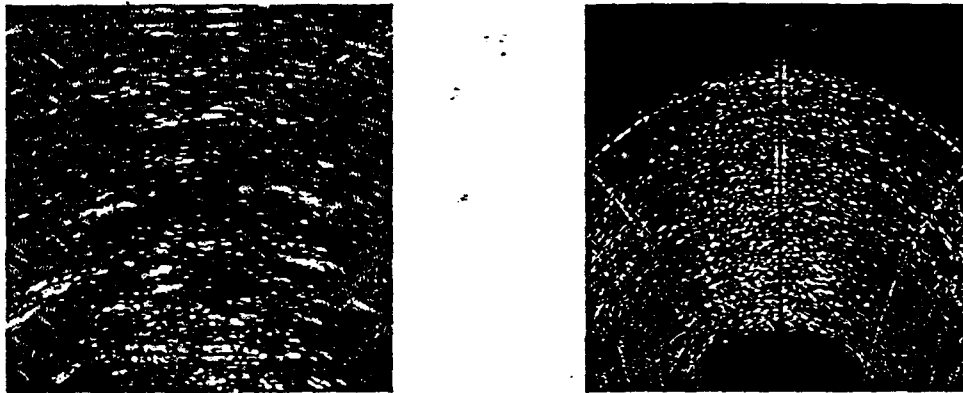

Figure 5. On the left, full-band, HH-polarization intensity image (clutter only, linear scale, 30 meters by 30 meters) and on the right, full-band, HH-polarization 2-D complex FFT intensity image (clutter only, linear scale, 512 by 512 pixels).

As an example, the procedure for obtaining the P-3 image is shown in figure 6. The 2-D complex FFT image (left), first has the aliasing removed (center), and then allows only the data with a frequency content ranging from 400 to 1000 MHz (right). The image on the right is converted back to the spatial domain by the inverse 2-D complex FFT. For each of the three airborne SAR sensors the procedure is the same except for the sensor bandwidth.
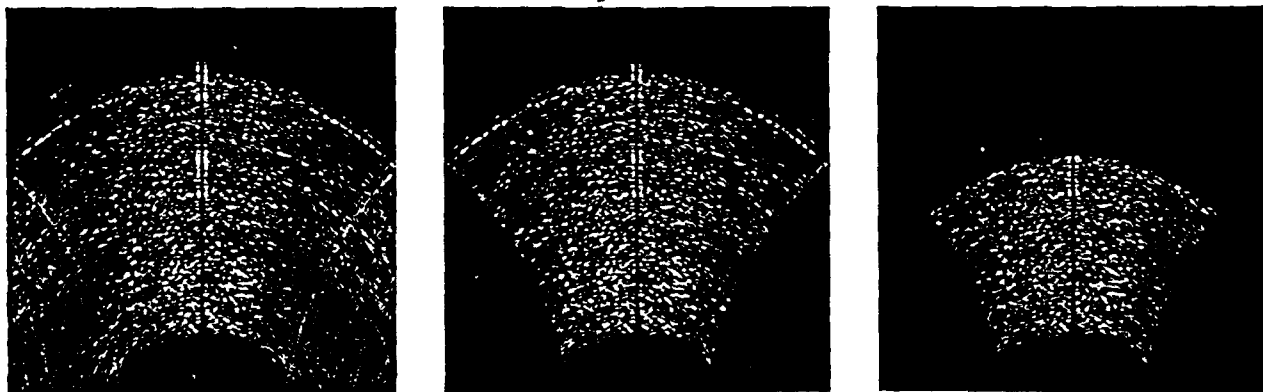

Figure 6. On the left, full-band, HH-polarization intensity image (clutter only, linear scale, 30 meters by 30 meters), in the center, aliasing removed, and on the right, 1000 to 1300 MHz data removed.

5. INCOHERENT CHANGE DETECTION DESCRIPTION

Change Detection is done by forming a normalized image of a scene with the target present, forming the normalized image of the same scene with only clutter, and after registration, the difference in the images is examined. Figure 7 and figure 8 show the full-band Rail SAR images that are to be evaluated for both HH- and VV-polarization, respectively. Mathematically, the image is formed by taking the envelope of the complex data pairs $(x = \sqrt{I^2 + Q^2})$, estimating the mean (μ_c) and standard deviation(σ_c) of the clutter after the targets and corner reflectors are suppressed, and forming the difference in the two images

$$\left[\frac{x - \mu_c}{\sigma_c}\right]_{H_1} - \left[\frac{x - \mu_c}{\sigma_c}\right]_{H_0} \tag{1}$$

H_1 represents the presence of the target and H_0 represents the absence of the target.
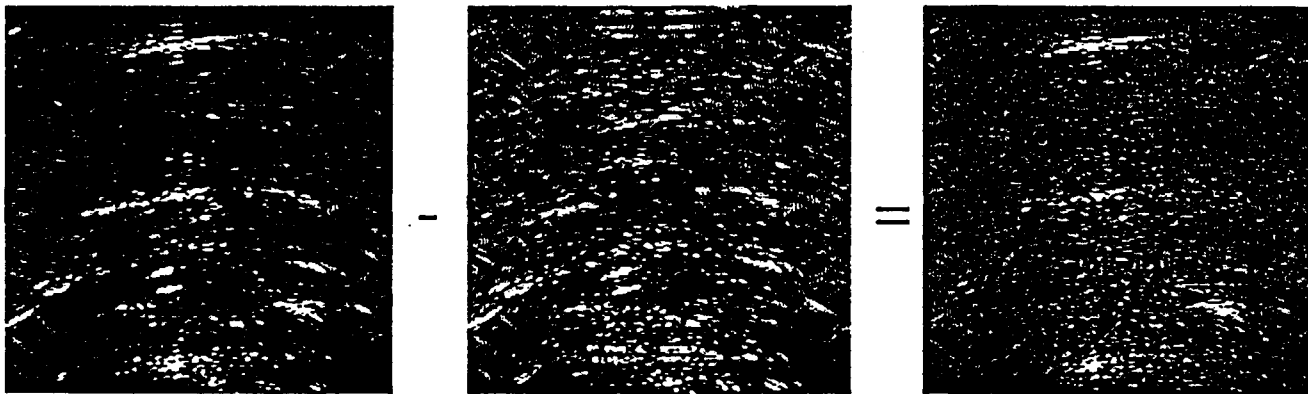

Figure 7. On the left, full-band, HH-polarization image (normalized intensity displayed on a linear scale with obscured truck and corner reflectors); in the center, full-band, HH-polarization image (normalized intensity displayed on linear scale with clutter only); and on the right, the difference between the image on the left and the image in the center.
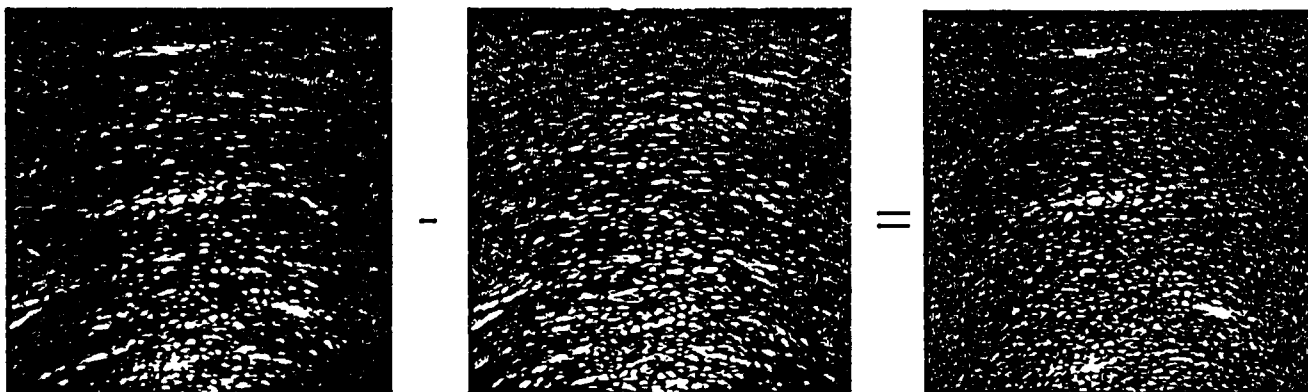

Figure 8. On the left, full-band, VV-polarization image (normalized intensity displayed on a linear scale with obscured truck and corner reflectors); in the center, full-band, VV-polarization image (normalized intensity displayed on linear scale with clutter only); and on the right, the difference between the image on the left and the image in the center.

6. SENSOR SIMULATED PERFORMANCE

Because only one target is being examined, performance curves such receiver operating characteristic (ROC) curves are not possible. To evaluate performance among the three simulated SAR sensors, the probability of false alarm versus threshold is displayed for each normalized intensity level image. The probability of false alarm is determined by ignoring the locations of the three corner reflectors and target (i.e. forming a 61 by 61 pixel mask centered around each location) and then generating a curve of one minus the cumulative probability of distribution of the remaining pixels. The target level is determined by placing a 61 by 61 pixel mask centered around the target location and recording the maximum pixel level. Normal detection refers to the examination of the image with the target present. Change detection refers to the examination of the differenced image.

Several performance curves appear below. They are organized by plotting the probability of false alarm versus threshold for each simulated sensor, parametric with normal detection and change detection, and with the left curve representing the HH-polarization and the right curve representing the VV-polarization. Figures 9, 10, and 11 show the results for the SRI UWBR, the Loral MSAR, and NAWC P-3, respectively. An * symbol is used to represent the target level response for normal detection and the # symbol is used to represent target response for change detection. Table 1 summarizes the target response and lists the target-to-clutter ratios.
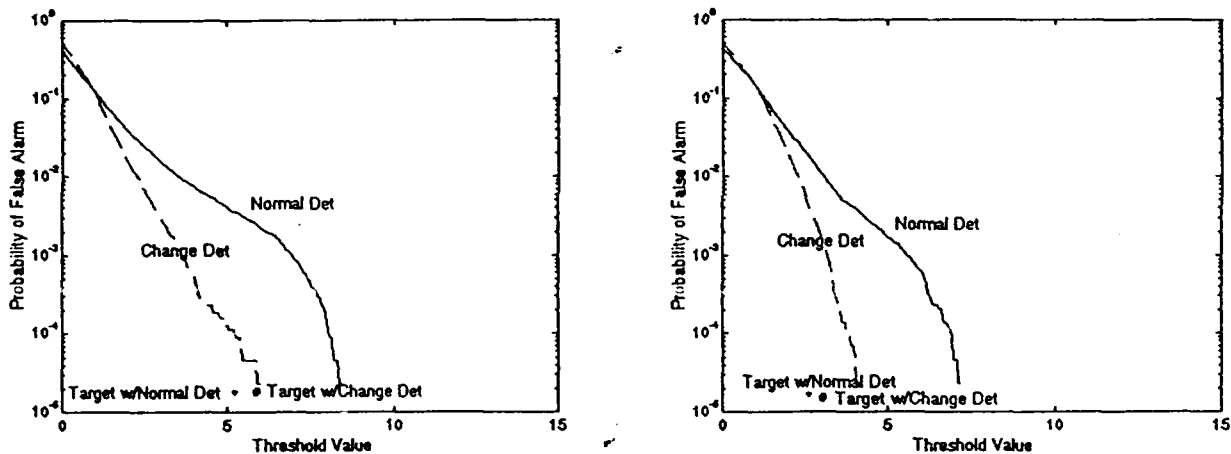

Figure 9. SRI UWBR (simulated high-band 400-600 MHz) probability of false alarm versus threshold for normal and change detection with HH-polarization (left) and VV-polarization (right).
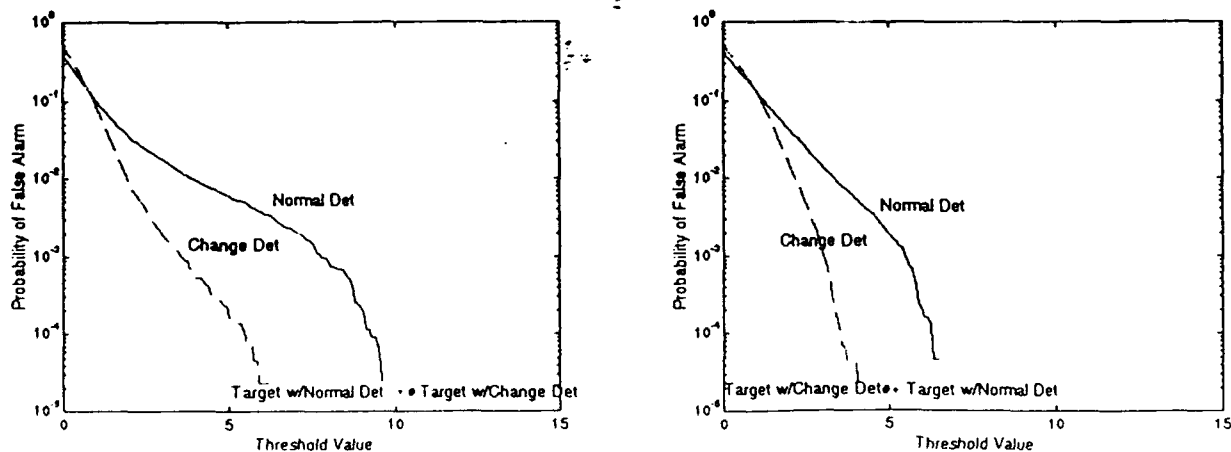

Figure 10. Loral MSAR (simulated band 500-800 MHz) probability of false alarm versus threshold for normal and change detection with HH-polarization (left) and VV-polarization (right).
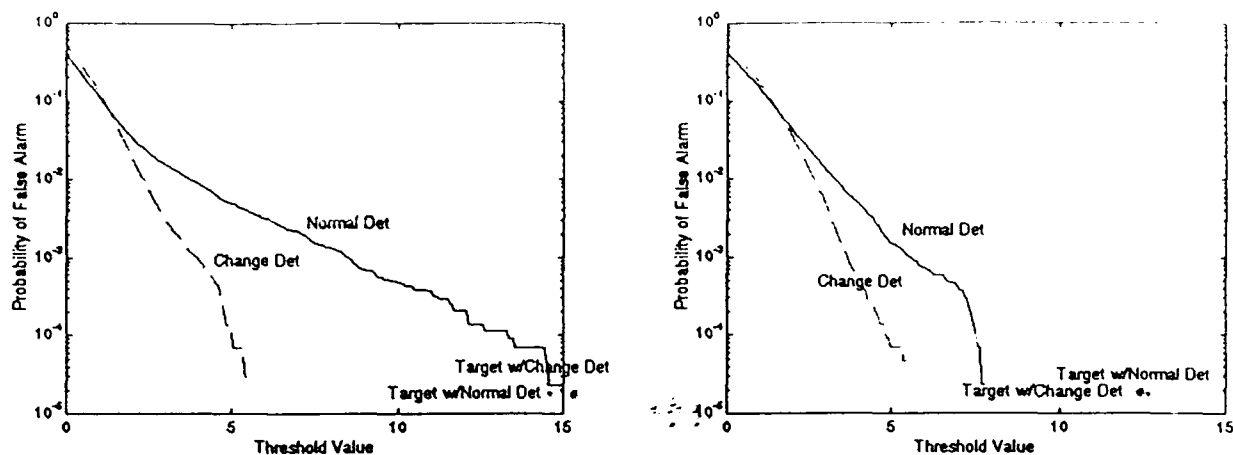
Figure 11. NAWC P-3 (simulated band 400-1000 MHz) probability of false alarm versus threshold for normal and change detection with HH-polarization (left) and VV-polarization (right).

Table 1: Target response information.

Sensor/Detection	Polarization	Target value	Clutter mean	Clutter variance	Target/clutter ratio (dB)
SRI UWBR/ Normal Det.	HH	5.17	-0.0215	0.910	14.11
SRI UWBR/ Normal Det.	VV	2.60	0.130	0.970	7.98
SRI UWBR/ Change Det.	HH	5.87	-0.172	1.108	15.18
SRI UWBR/ Change Det.	VV	3.05	-0.108	0.981	10.08
Loral MSAR/ Normal Det.	HH	10.18	-0.061	0.527	22.99
Loral MSAR/ Normal Det.	VV	5.09	0.298	0.758	14.82
Loral MSAR/ Change Det.	HH	10.53	-0.076	0.812	21.42
Loral MSAR/ Change Det.	VV	5.01	0.088	1.151	13.24
NAWC P-3/ Normal Det.	HH	14.48	-0.065	0.550	25.85
NAWC P-3/ Normal Det.	VV	13.06	0.339	1.085	21.74
NAWC P-3/ Change Det.	HH	15.18	-0.098	0.976	23.78
NAWC P-3/ Normal Det.	VV	12.65	0.151	1.381	20.53

Figure 9 compares normal detection to change detection for the high band SRI sensor. Notice that change detection works substantially better than normal detection in reducing false alarms. However, change detection does not completely eliminate the false alarm level. This is due to the lack of high clutter correlation as seen in Table 2. Because the target is off cardinal angle (24 degrees off broadside relative to the Rail SAR) and obscured by the foliage, the target level relative to the false alarms is marginal. Target detection level is slightly better for change detection than with normal detection. Change detection appears to both improve false alarms and target detection level. As the bandwidth is increased as shown in figures 10 and 11, the false alarm level progressively increases and the effective of change detection is more dramatic. In addition, the target level progressively increases. The NAWC P-3 shows considerably better performance than the high band SRI UWBR using change detection. For normal detection, the relationship of false alarms to target level indicates that the Loral MSAR sensor works best, at least for HH-polarization.

Table 2: Clutter correlation coefficients depending on frequency band.

Sensor	Frequency Band (MHz)	HH-polarization correlation coefficient	VV-polarization correlation coefficient
SRI	400-600	0.59	0.54
MSAR	500-800	0.67	0.56
P-3	400-1000	0.57	0.45
Full-band (no aliasing)	400-1300	0.47	0.31
Full-band (aliasing)	400-1300	0.35	0.20

Comparing the sensors by detection type, figures 12 and 13, show some interesting results. For normal detection using HH-polarization, when the frequency band is increased as represented by the sensor types, the false alarm and target return progressively increase and the MSAR sensor gives the best relationship of false alarm to target return. However, for normal detection and VV-polarization, the P-3 shows a very good relationship of false alarm to target return. When looking at figure 13, change detection, the false alarm distributions are very similar for each sensor while the target return level increases as the bandwidth is increased. This implies that the P-3 sensor should do very well using change detection.
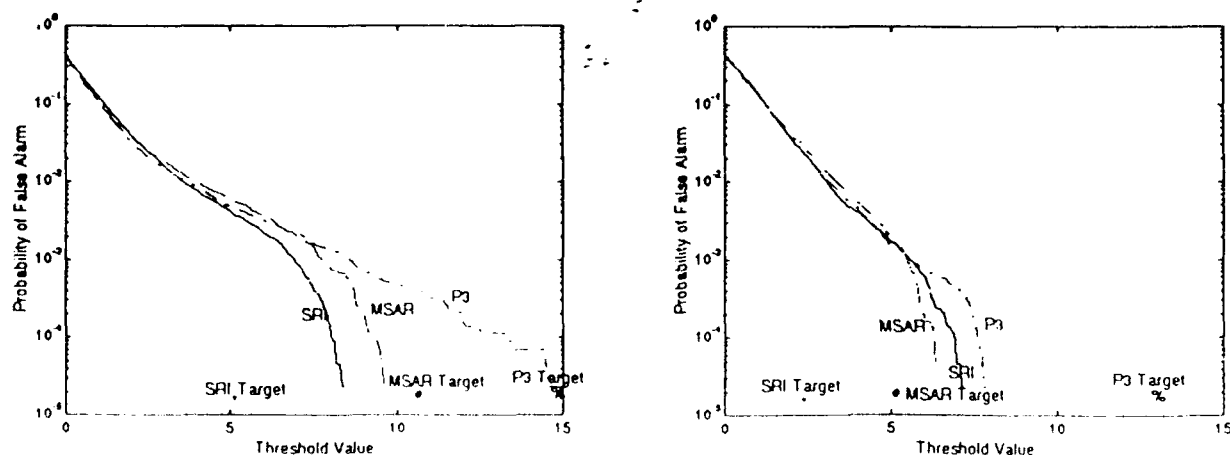

Figure 12   Sensor comparison using normal detection with HH-polarization on the left and VV-polarization on the right.
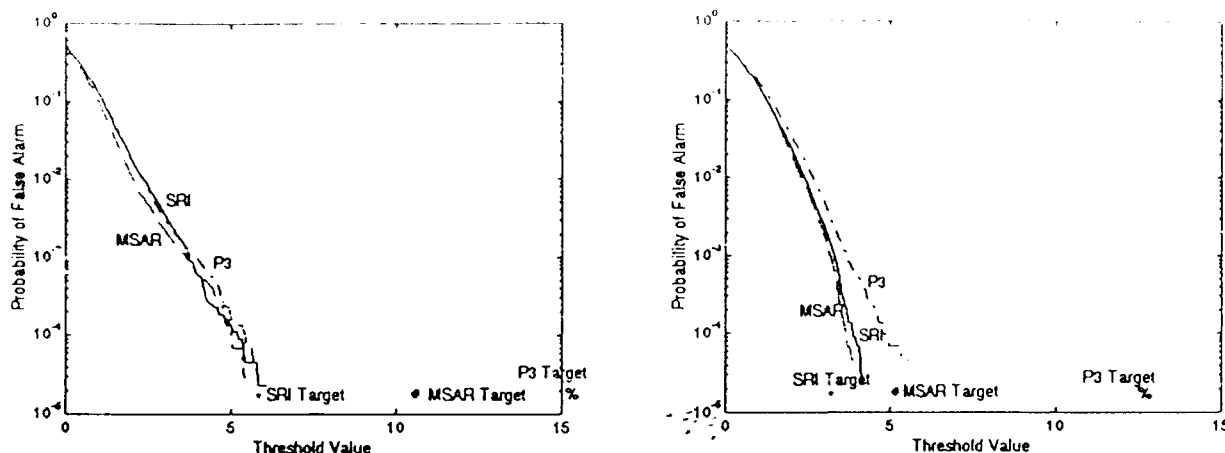
Figure 13. Sensor comparison using change detection with HH-polarization on the left and VV-polarization on the right.

7. OBSERVATIONS AND CONCLUSIONS

An investigation of the effectiveness of frequency band on detecting an obscured vehicle in foliage using the ERIM Rail SAR was conducted. Three FOPEN SAR sensors were simulated through frequency filtering of two images, (1) having an obscured vehicle in the scene and (2) the same scene with the vehicle removed. This allowed a comparison in performance using change detection. Observations indicated that for normal detection, false alarms and target detection levels generally increase with increasing bandwidth. Using change detection, false alarm distributions are greatly reduced when compared to normal detection, and the distributions are very similar over the three operating bandwidths considered. However, even better target detection level performance using change detection occurred as the operating bandwidth increased. This indicates that a large bandwidth sensor such as the NAWC P-3 sensor would be very attractive for change detection.

8. ACKNOWLEDGEMENTS

Special thanks goes to Larry Stotts of ARPA for providing the catalyst to formulate the idea to do this analysis, to Juan Roman of the Air Force for making the data available to NCCOSC RDT&E Division, to Terry Lewis and Sue Wei of ERIM for providing follow-up information regarding the ERIM Rail SAR experiment, and to Chris Yerkes, Kristine Hironaka, and Diana Ly of NCCOSC RDT&E Division whose help made this article possible.

9. REFERENCES

1. James, R. and L. Hoff, "Investigation of SAR Target Detection Algorithms using Narrowband and Ultra Wideband Sensors," *Proceedings of the Third Automatic Target Recognizer Systems and Technology Conference*, 29 June -1 July 1993, Naval Post Graduate School, Monterey, CA, *Volume 1, GACIAC I R-93-01*, pp. 327-340.

2. Sheen, D., S. Wei, T. Lewis, and S De Graaf, "Ultrawide bandwidth polarimetric SAR imagery of foliage-obscured objects," *SPIE Vol. 1875 Ultrahigh Resolution Radar (1993)*, 20 January, 1993, Los Angeles, CA, pp. 106-113.

3. Lewis, T. and D. Sheen, "Concealed Target Detection under Foliage or Underground," Environmental Research Institute of Michigan, Ann Arbor, MI, unpublished and undated viewgraph presentation.